Title

Patient-specific alterations in blood plasma cfRNA profiles enable accurate classification of cancer patients and controls

Authors

Annelien Morlion (1,2), Philippe Decruyenaere (1,2,3), Kathleen Schoofs (1,2,4), Jasper Anckaert (1,2), Justine Nuytens (1,2), Eveline Vanden Eynde (1,2), Kimberly Verniers (1,2), Celine Everaert (4), Fritz Offner (3), Jo Van Dorpe (5), Jo Vandesompele° (1,2), Pieter Mestdagh°* (1,2)

(1) Department of Biomolecular Medicine, Ghent University, Ghent, Belgium

(2) OncoRNALab, Cancer Research Institute Ghent (CRIG), Ghent, Belgium

(3) Department of Hematology, Ghent University Hospital, Ghent, Belgium

(4) TOBI Lab, Center for Medical Biotechnology, VIB-UGent, Zwijnaarde, Belgium

(5) Department of Pathology, Ghent University Hospital, Ghent, Belgium

°Both authors contributed equally to this work

*Corresponding author

Author contributions

Conceptualization: AM, CE, JV, PM

Data Curation: AM

Funding acquisition: AM, JV, JVD, PM

Software: AM, JA

Validation: AM

Formal analysis: AM

Investigation: EV, JN, KV

Methodology: AM, JV, PM

Project administration: AM, JV, PM

Resources: FO, JV, JVD, KS, PD, PM

Supervision: JV, PM

Visualization: AM

Writing – original draft: AM, JV, PM

Writing – review & editing: all authors

Abstract

Circulating nucleic acids in blood plasma form an attractive resource to study human health and disease. Here, we applied mRNA capture sequencing of blood plasma cell-free RNA from 266 cancer patients and cancer-free controls (discovery n=208, 25 cancer types; validation n=58, 3 types). We observed cancer-type specific as well as pan-cancer alterations in cell-free transcriptomes compared to controls. Differentially abundant RNAs were heterogenous among patients and among cohorts, hampering identification of robust cancer biomarkers. Therefore, we developed a novel method that compares each individual cancer patient to a reference control population to identify so-called biomarker tail genes. These biomarker tail genes discriminate ovarian, prostate, and uterine cancer patients from controls with very high accuracy (AUC = 0.980). Our results were confirmed in additional cohorts of 65 plasma donors (2 lymphoma types) and 24 urine donors (bladder cancer). Together, our findings demonstrate heterogeneity in cell-free RNA alterations among cancer patients and propose that case-specific alterations can be exploited for classification purposes.

Introduction

Cancer is a complex disease with considerable heterogeneity, both between as well as within cancer types. Finding robust and easily accessible biomarkers is crucial to improve patient well-being and outcome. Such biomarkers can either assist in early detection of cancer, enabling treatment to start at an earlier stage, or they can support diagnosis, treatment selection or response monitoring. As an alternative for biomarkers that require invasive tissue biopsies, liquid biopsy-based biomarkers such as circulating nucleic acids have emerged as a promising tool for cancer diagnosis and monitoring.

To date, most studies on circulating nucleic acids in cancer patients have focused on circulating tumor DNA (ctDNA). The amount of tumor DNA in circulation is highly dependent on the tumor type and burden[1], suggesting that ctDNA can be less informative for certain cancer types or early-stage cancers. Cell-free RNA (cfRNA) may complement ctDNA by reflecting dynamic changes in gene expression during cancer development and progression, or upon treatment, in both healthy and diseased cells. A recent study showed that different

cell types contribute RNA to the healthy cell-free plasma transcriptome, and that cfRNA allows monitoring of cell-type-specific changes in diseases, such as non-alcoholic fatty liver and Alzheimer's disease[2]. The potential of cfRNA as prognostic biomarker has also been demonstrated for pre-eclampsia and organ damage in pregnancy[3]. Some studies have also shown potential of using cfRNA biomarkers in certain cancer types[4–6]. Larson et al.[4] specifically looked at genes that are "dark" (no or few detected transcripts) in plasma from healthy controls but abundant in plasma from lung and/or breast cancer patients and found indications of tissue-of-origin signal. Chen et al.[5] reported potential of combining human and microbe-derived plasma cfRNA for distinguishing healthy donor and cancer plasma samples (colorectum, stomach, liver, lung, and esophageal cancer) based on profiles of RNAs showing group-level differences. Roskams-Hieter et al.[6] showed plasma cfRNA classification potential for liver cancer and multiple myeloma patient samples compared to non-cancer controls, with a higher accuracy using learning vector quantization feature selection compared to group-level differential abundance. The authors, however, indicated that liver and bone marrow are major contributors to the plasma transcriptome which may result in more cancer signal.

Here, we further examined the impact of different cancer types on plasma cfRNA profiles in different cohorts (**Table 1**). We first quantified cell-free mRNAs in different cohorts of blood plasma from cancer patients with locally advanced or metastatic tumors and cancer-free donors to uncover tumor or tissue-of-origin mRNA signatures with diagnostic potential. Results revealed substantial heterogeneity in cell-free mRNA abundance among cohorts, questioning the biomarker potential of cell-free mRNA signatures. However, patient-specific alterations, reflected by the number of cell-free mRNAs with differential abundance in a patient sample compared to a cancer-free control population, enabled to accurately distinguish cancer patients from healthy individuals.

Table 1: Cohort overview. Name, number of donors (one sample per donor), biofluid type, library preparation method and application of the cohort in this study. (*) eight control donors also included in pan-cancer cohort, data of these donors not used for validation analyses (see Methods).

cohort name	cancer patients (cancer types)	controls	biofluid	library preparation	application
pan-cancer cohort	200 (25)	8	plasma	mRNA capture (Illumina DNA Prep with Enrichment)	discovery
three-cancer cohort	36 (3)	30*	plasma	mRNA capture (Illumina DNA Prep with Enrichment)	validation pan-cancer analyses & discovery tail gene concept

lymphoma cohort	43 (2)	22	plasma	total RNA (SMARTer Stranded Total RNA-Seq Kit v3 - Pico Input Mammalian)	validation tail gene concept
bladder cancer cohort	12 (1)	12	urine	mRNA capture (TruSeq RNA Exome)	validation tail gene concept

Results

A diverse repertoire of cell-free mRNAs in plasma

To characterize the blood plasma cell-free mRNA transcriptome, we collected blood plasma from a pan-cancer discovery cohort consisting of 208 individuals covering 25 different cancer types and aged-matched healthy controls (**Figure 1**a, Supplemental Table 1). MRNA capture sequencing of the pan-cancer plasma cohort resulted in 3 to 56M paired-end reads per sample (median 16M) after quality filtering with no significant differences among groups (Kruskal-Wallis test p>0.05) (Supplemental Figure 1). On average 84% (95% CI [82.59, 84.66]) of uniquely mapped reads were assigned to protein coding genes and most other reads originated from mitochondrially encoded ribosomal RNAs (Supplemental Figure 2). Per sample, between 7439 and 13,039 unique mRNAs (median 10,932) were detected with at least 10 counts – we use the term mRNA to refer to all mRNA reads mapping to the same gene (**Figure 1**b). All plasma samples had 5263 mRNAs in common and 9908 mRNAs were found in at least 75% of the samples. Of note, we detected more mRNAs in plasma from acute myeloid leukemia (AML) patients compared to plasma from controls and from patients with solid cancers (Kruskal-Wallis p=6.6E-4, effect size= 0.163, post hoc two-sided Wilcoxon rank-sum q < 0.05 for AML vs controls and 16 out of 24 solid cancer types). Although some AML samples were sequenced deeper, sequencing depth alone did not explain the higher number of detected mRNAs (Supplemental Figure 3). We next determined the mRNA concentration using synthetic RNA spikes that were added to each lysed plasma sample (**Figure 1**c). MRNA concentrations ranged from 0.003 to 8.302 ng/ml with an average concentration of 0.486 ng/ml. Despite the higher number of detected mRNAs, the mRNA-concentration in AML plasma was not significantly higher than controls or other cancer types. Moreover, though the largest median mRNA concentration (READ, 0.648 ng/ml) was more than 10 times higher than the smallest median (ANA, 0.063 ng/ml), no significant concentration differences were found between the groups (Kruskal-Wallis test p=0.0275, effect size=0.087, with all post hoc two-sided Wilcoxon rank-sum q > 0.05). Besides the small sample sizes, this may be related

to the considerable cfRNA concentration variability between patients, which is also reported at cfDNA level[7].

We then searched for evidence of tumor-derived cfRNA by investigating known cancer fusion transcripts in individual plasma samples. In every cancer plasma sample, we only considered fusion transcripts that had been documented in tumor tissue of that same cancer type. Such fusion transcripts were only identified in plasma samples of AML patients. The PML::RARA fusion transcript[8] was found in two AML plasma samples with several reads supporting the fusion (7 to 19 spanning pairs and 6 to 9 unique spanning reads). The reciprocal RARA::PML fusion was found in one of both AML plasma samples (19 pairs and 17 unique reads). In plasma samples of solid cancer types, we only detected fusion transcripts that had not been reported in the tumor tissue of these cancer types (Supplemental Table 2). Of note, these fusion transcripts had fewer supporting reads (1 to 2 pairs and 2 to 5 unique reads) than the PML::RARA/RARA::PML fusions in AML and may thus represent false positives. Moreover, other fusions with few supporting reads were also identified in healthy control plasma samples. While the two AML samples with the PML::RARA fusion transcripts were sequenced deeper than other samples, the fusions were still detected when downsampling to the median number of reads of the pan-cancer cohort. These analyses confirm the presence of tumor cell-derived cfRNA in plasma samples from AML patients.
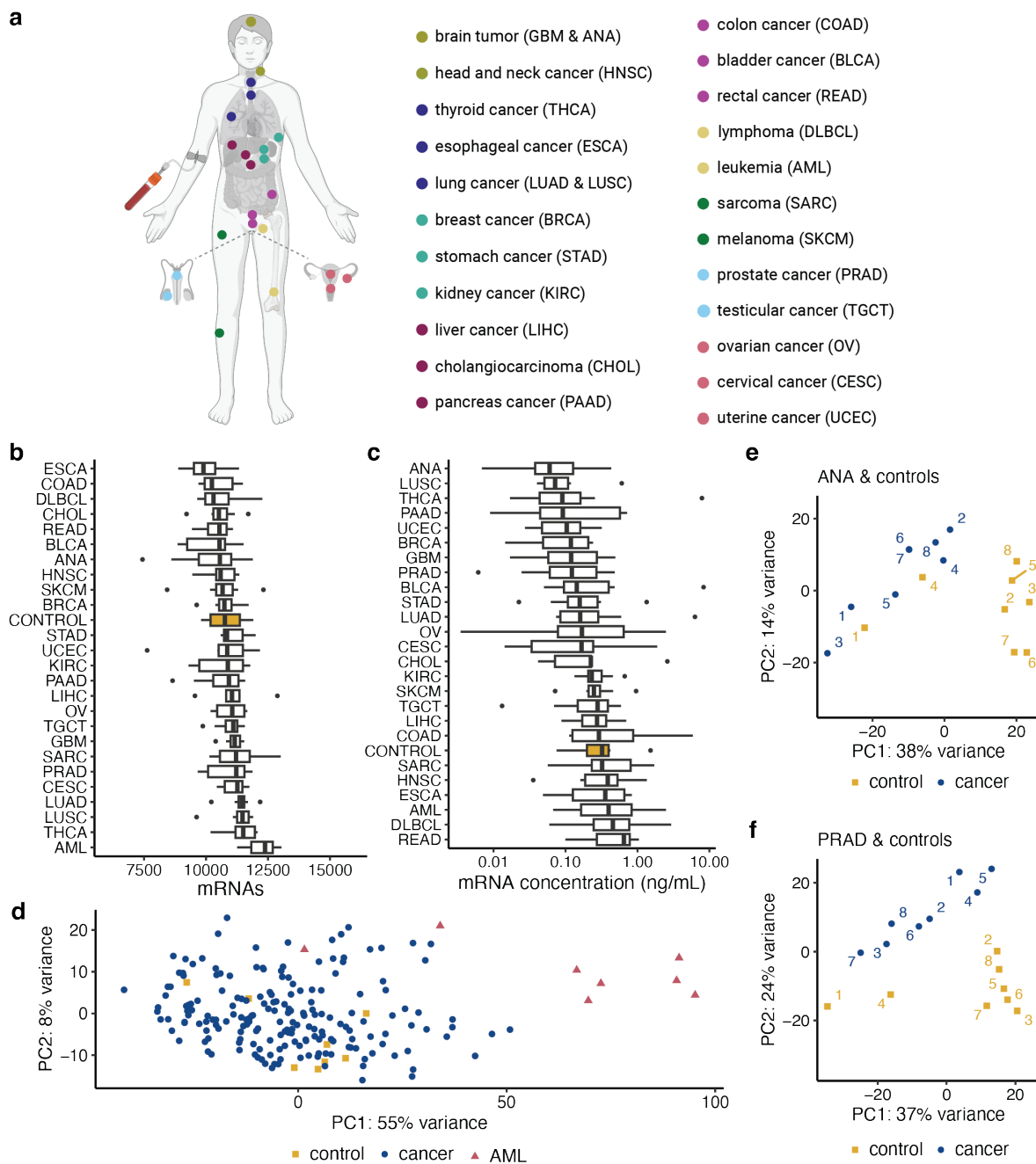
Figure 1: Pan-cancer plasma cohort overview, mRNA content and sample clustering. a, *Primary sites of the 25 cancer types in the pan-cancer cohort. Primary sites are indicated with colored dots and corresponding cancer types are listed (top to bottom) with the (sub)type abbreviations between brackets. Full names and more details can be found in Supplemental Table 1.* ***b,*** *Number of plasma mRNAs, detected with at least 10 counts, across cancer types and healthy controls. Groups ordered according to median.* ***c,*** *Variability in plasma mRNA concentration across cancer types and healthy controls. Groups ordered according to median.* ***b*** *and* ***c,*** *Boxplots show lower quartile (Q1), median, and upper quartile (Q3). Whiskers extend from the lower and upper quartile to the smallest and largest value, respectively, within at most 1.5*interquartile range (Q3-Q1) from that quartile. More extreme points are plotted as individual dots.* ***d,*** *Principal component analysis using the 500 most variable mRNAs in the pan-cancer cohort (with variance stabilizing transformation DESeq2). Yellow squares: control*

*samples; red triangles: acute myeloid leukemia samples; blue dots: non-leukemia cancer samples. **e** and **f**,*
Principal component analysis using the 500 most variable mRNAs in controls and anaplastic astrocytoma (ANA)
or prostate cancer (PRAD) patients, respectively. Replicate numbers are indicated in the plot. PC: principal
component.

Differential mRNA abundance in cancer patients' plasma compared to controls

Principal component analysis revealed a clear separation between AML and other plasma samples for six out of eight AML patients (**Figure 1**d). Control samples mostly clustered in between samples of solid tumors. Analysis of individual solid tumor types revealed that most patient samples could be separated from controls in the first two principal components (**Figure 1**e and f, Supplemental Figure 4), suggesting that plasma cfRNA profiles of cancer patients differ from that of controls.

Differentially abundant mRNAs were identified in every cancer-control comparison, with numbers varying from 10 to 2583 (median 128) for higher abundant mRNAs and from 89 to 2727 (median 221) for lower abundant mRNAs in cancer compared to control (**Figure 2**a). Most differentially abundant mRNAs were found in AML (5310 mRNAs), followed by uterine cancer (UCEC) and sarcoma (SARC) with 1154 and 763 mRNAs, respectively. Head and neck (HNSC), rectal (READ) and breast cancer (BRCA) had the lowest number of differentially abundant mRNAs (127, 136, and 145 respectively).

In total, 6758 unique mRNAs were differentially abundant in one or more cancer-control comparisons (b) and the median absolute fold change was 3.1. One quarter of differentially abundant mRNAs had an absolute fold change of at least 4.6. Hierarchical clustering based on differential mRNA abundance mostly separated cancer and control samples but also revealed variability in gene abundance within groups (**Figure 2**b and c, Supplemental Figure 5).

4442 mRNAs (66%) were differentially abundant in one cancer type only (**Figure 2**d), and most (3680 mRNAs) were identified in AML. While many mRNAs were differentially abundant in plasma of only one or a few cancer types, 26 differentially abundant mRNAs were recurrent in 23 out of 25 cancer-control comparisons (**Figure 2**d). These mRNAs were all lower abundant

in cancer compared to controls and showed enrichment for inflammatory and immune response pathways (Supplemental Table 3).
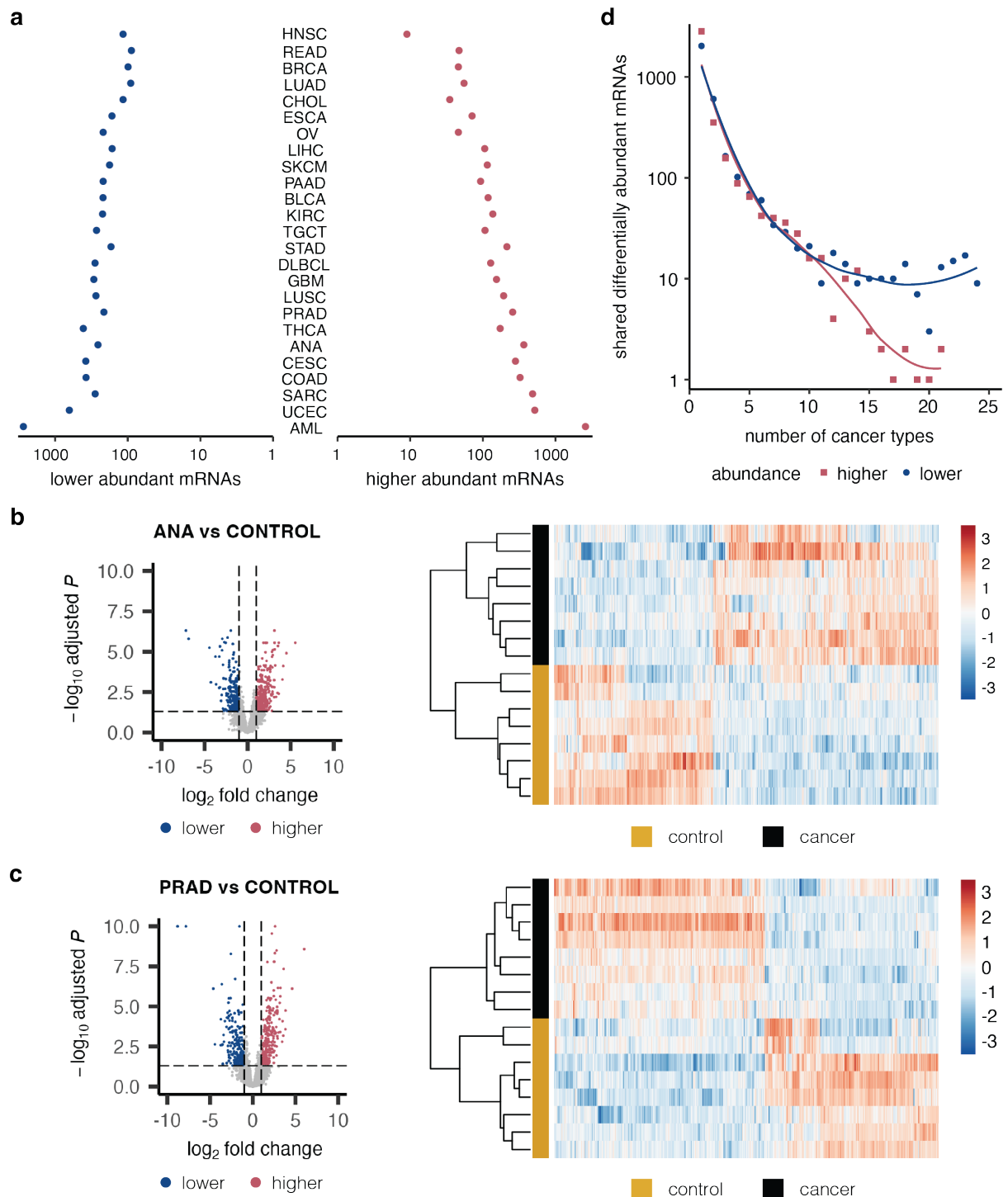

Figure 2: Differentially abundant mRNAs in cancer versus control. a, *Differentially abundant mRNAs in plasma from cancer patients versus controls. Cancer types ordered based on total number of differentially abundant mRNAs (q < 0.05 and |log₂ fold change|>1).* **b** *and* **c,** *Volcano plot and heatmap of differentially abundant mRNAs in anaplastic astrocytoma vs controls (**b**) and in prostate cancer vs controls (**c**). Volcano plots have a horizontal*

*line at q = 0.05 and vertical lines at log$_2$ fold change of -1 and 1, resp. Higher (red): higher abundant in cancer compared to control samples (q < 0.05 and log$_2$ fold change > 1); lower (blue): lower abundant in cancer compared to control samples (q < 0.05 and log$_2$ fold change < -1). Heatmaps show relative abundance of differentially abundant mRNAs (columns) in individual plasma samples (rows) based on log2(normalized counts+1) followed by z-score transformation per gene. Clustering of genes and samples based on Pearson correlation. **d,** Recurrence of differentially abundant mRNAs (shown in a) across cancer types.*

Enrichment of pathways and cell types in cancer patients' plasma

To explore the pathways, cell types and tissues underlying the differentially abundant mRNAs in cancer plasma, we first applied gene set enrichment analyses using hallmark[9], Kyoto Encyclopedia of Genes and Genomes (KEGG)[10], and custom tissue- and cell type gene sets (**Figure 3**a, Supplemental Figure 6a and b). We observed a negative enrichment of various immune-related signals (interleukin signaling, interferon gamma and inflammatory response, and neutrophils) across all cancer types except UCEC, with q<0.05 in at least 21 out of 25 cancer types. 'Ribosome' was also negatively enriched in all solid cancer types (q<0.05 in 19 out of 24 types). These results are in line with a previous study by Chen et al.[5] on plasma cfRNA profiles of five early-stage solid cancer types. Other negatively enriched gene sets with q<0.05 in at least half of the cancer types in our cohort were 'epithelium' and 'blood' related. Conversely, 'extracellular matrix receptor' and 'focal adhesion' gene sets were significantly positively enriched in at least half of the cancer types, confirming results by Chen et al. Other positively enriched gene sets included 'epithelial-mesenchymal transition', 'vasculature', 'adipose tissue', 'brain', and 'hematopoietic stem cells'.

Cancer type-specific enrichment of cfRNA reflecting the primary tumor site was only observed for liver cancer patients. 'Liver tissue', 'liver cancer tissue', and 'hepatocyte' gene sets were all positively enriched in liver cancer patients' plasma (q<0.05, **Figure 3**b) and not in plasma from any other cancer type. A 'bronchial epithelial cells' gene set was significantly enriched in lung adenocarcinoma and lung squamous cell carcinoma (LUAD q=0.027; LUSC q=0.026), but this enrichment was also found in four other cancer types (ANA, CESC, CHOL, and UCEC). We then applied computational deconvolution to enumerate the cell type fractions contributing to plasma cfRNA profiles (Supplemental Table 4). Platelets, erythrocytes/erythrocyte progenitors, monocytes, macrophages, and B-cells formed the top-5 of most abundant cell types that contributed to plasma cfRNA of both controls and patients

with solid tumors (**Figure 3**c). Except for macrophages, these cell types were also reported as the most abundant cell types in a previous study on healthy donor plasma[2]. Plasma from AML patients showed a very different composition. Several cell types - including hematopoietic stem cells, myeloid progenitor cells, and monocytes - were increased or even exclusively present in AML plasma samples, in line with the blood cell counts typically observed in these patients[11]. Myeloid progenitor cells, normally not present in peripheral blood, were the second most abundant cell type in the AML plasma samples (mean 10.7%), with almost no signal in other plasma samples (mean 0.1%) (Supplemental Figure 7). Moreover, the platelet fraction in AML plasma was significantly lower compared to other groups (two-sided Wilcoxon rank sum p=3.8E-5, effect size=0.289) with on average 18.3% in AML compared to 62.3% in other samples, reflecting the reduced thrombocyte counts commonly found in leukemia patients[11].

In plasma from patients with solid tumors, the platelet fraction was significantly higher compared to controls (Supplemental Figure 7, two-sided Wilcoxon rank-sum p=2.3E-2, effect size=0.163), which is in line with the prognostic value of platelet counts and the frequent occurrence of thrombocytosis in solid tumor patients[12,13]. For neutrophils, erythrocyte/erythroid progenitor cells, thymocytes, and T-cells, the fraction was significantly lower in cancer patients' plasma compared to controls (two-sided Wilcoxon rank-sum p=1.8E-2 (effect size=0.169), p=1.4E-2 (effect size=0.176), p=1.8E-2 (effect size=0.164), p=4.3E-4 (effect size=0.252), respectively).
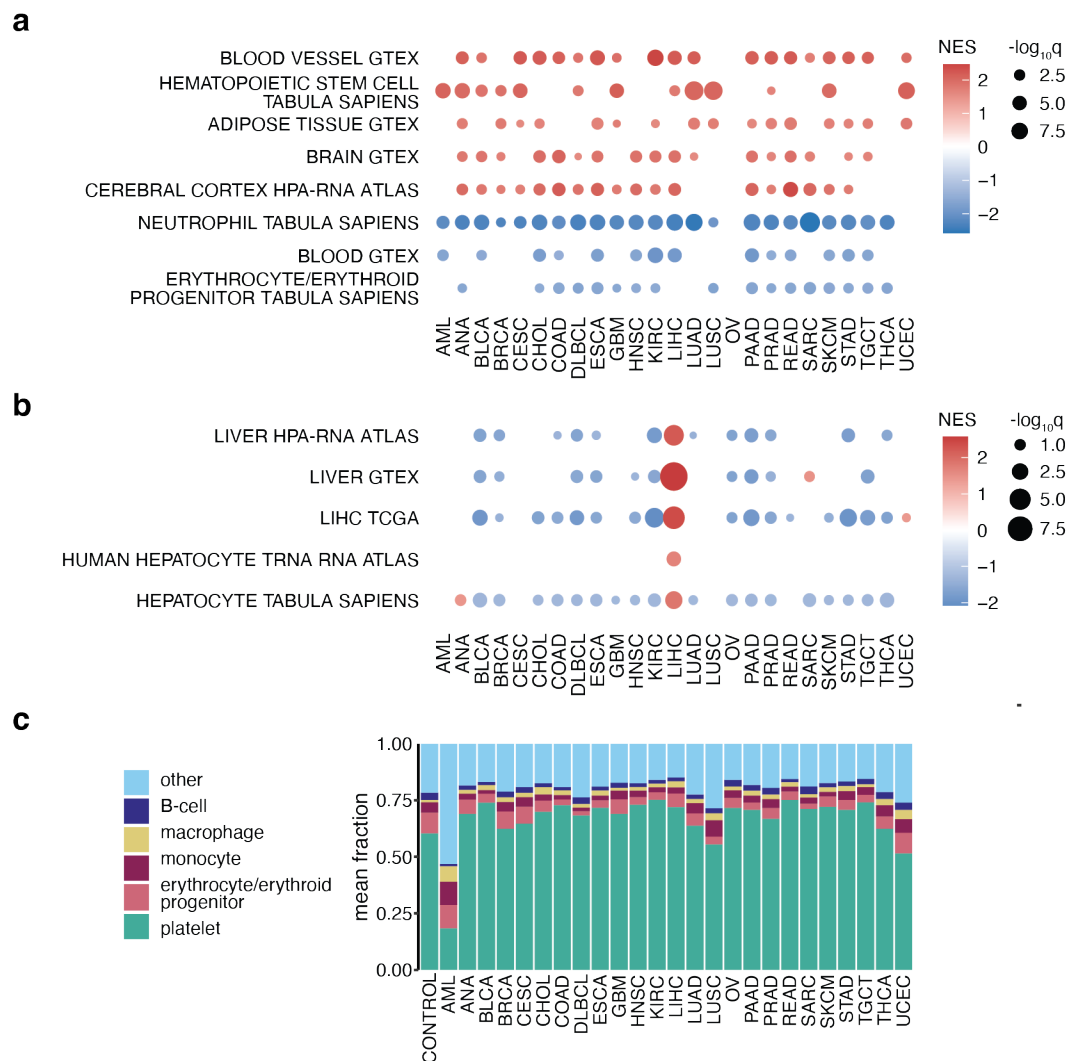
Figure 3: Gene set enrichment and cell type deconvolution reveal pan-cancer and cancer-type specific signals. a, Gene set enrichment analysis results for custom tissue and cell type sets. Only sets that are significantly enriched in at least half of the cancer types are shown. Gene sets with q < 0.05 colored according to normalized enrichment scores (NES). b, Liver-related gene set enrichment in plasma from liver cancer patients, gene sets with q < 0.25 colored according to NES. Detailed information about gene sets can be found in Methods. c, Average fraction of the five most abundant cell types based on deconvolution. Other: cumulative sum of other cell types. The five most abundant cell types were selected based on mean ranking in all groups.

Independent validation cohort confirms systemic signal and cfRNA heterogeneity

To validate our findings, we processed an independent (three-cancer) cohort of plasma samples which, after removing samples with low read depth, included samples from 20 cancer-free control donors and 35 cancer patients with one of three different solid cancer types: prostate (PRAD, n=12), ovarian (OV, n=11), and uterine (UCEC, n=12) cancer. 7 to 61M paired-end reads were obtained per sample (median 28M) with no significant difference in

sequencing depth among groups (Kruskal-Wallis p=0.7858) (Supplemental Figure 8a). In line with the pan-cancer cohort, we detected between 8642 and 11,944 mRNAs per sample (Supplemental Figure 8b), with 6194 mRNAs shared across all plasma samples of this three-cancer cohort. MRNA concentrations ranged from 0.007 to 0.414 ng/ml (Supplemental Figure 8c).

Most cancer samples could be separated from controls in the first principal component, especially for prostate and ovarian cancer (**Figure 4**a). Based on differential abundance analyses between cancer and control samples, we found the highest number of differentially abundant mRNAs in OV (995 higher abundant, 1644 lower abundant), followed by PRAD (848 higher abundant, 1043 lower abundant) (**Figure 4**b). The lowest number of differentially abundant mRNAs was found for UCEC (243 higher abundant, 349 lower abundant) even though this cancer type had the most differentially abundant mRNAs in the pan-cancer cohort. Hierarchical clustering based on differential mRNA abundance in this three-cancer cohort mostly separated cancer and control samples but again revealed variability in mRNA abundance within groups (Supplemental Figure 9).

189 and 299 mRNAs were significantly higher and lower abundant, respectively, in plasma from all three cancer types compared to controls (**Figure 4**b). The lower abundant mRNAs included all 26 mRNAs that were identified as lower abundant in most cancers in the pan-cancer cohort. There was a significant, although limited, overlap in differentially abundant mRNAs between the three-cancer and the pan-cancer cohort for each of the three cancer types (Fisher's exact test on lower abundant mRNAs: OV p=8.4E-118 (odds ratio=30.0), PRAD p=1.1E-155 (odds ratio=59.3), UCEC p=7.6E-13 (odds ratio=4.2); on higher abundant mRNAs: OV p=4.0E-4 (odds ratio=4.6), PRAD p=2.9E-52 (odds ratio=12.2), UCEC p=2.2E-5 (odds ratio=3.3); Jaccard index [0.9-14.3%]) (**Figure 4**c and Supplemental Figure 10a). Respectively 38%, 49%, and 95% of the differentially abundant mRNAs in OV, PRAD, and UCEC in the pan-cancer cohort could not be confirmed in the three-cancer cohort. Notably, mRNAs with lower abundance showed a higher overlap between both cohorts than mRNAs with higher abundance.

In line with the pan-cancer cohort, there was no enrichment of cancer type specific gene sets reflecting tumor tissue of origin in the OV, PRAD and UCEC samples in the three-cancer cohort. However, enriched gene sets shared among at least half of the cancer types in the

pan-cancer cohort were confirmed in the three-cancer cohort, except for adipose tissue (**Figure 4**d, Supplemental Figure 10b and c).

Cell type deconvolution confirmed platelets, erythrocyte/erythroid progenitor cells, monocytes and B-cells among the top-5 cell types contributing cfRNA to plasma (**Figure 4**e, Supplemental Table 4), with neutrophils being ranked as the fourth most abundant cell type. The higher platelet fraction in cancer patient plasma was even more pronounced in the three-cancer cohort (two-sided Wilcoxon rank-sum cancer versus control p=5.8E-9, effect size= 0.679), especially for ovarian and prostate cancer (Supplemental Figure 11). Neutrophils, erythrocyte/erythroid progenitor cells, thymocytes and T-cells again had a lower plasma fraction in cancer patients compared to controls (two-sided Wilcoxon rank-sum p=4.4E-6 (effect size=0.556), p=3.2E-7 (effect size=0.610), p=6.4E-5 (effect size=0.419), p=4.1E-2 (effect size=0.261), respectively).

Taken together, the limited overlap of differentially abundant mRNAs between the pan-cancer and three-cancer cohort highlights plasma transcriptome variability, yet enrichment and cell type contribution analyses confirm the systemic cfRNA changes in plasma from cancer patients.
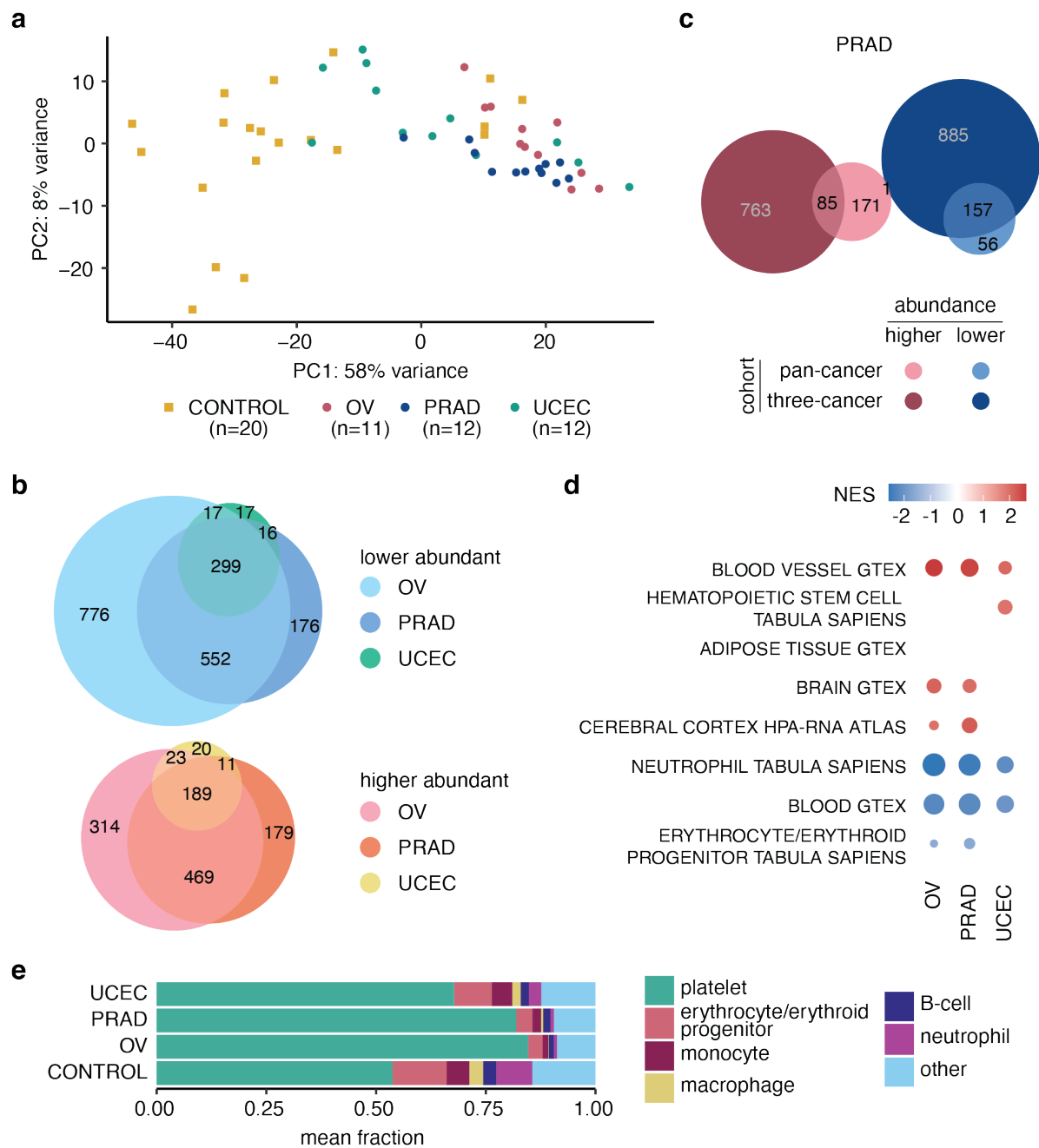
Figure 4: Three-cancer cohort confirms findings from pan-cancer cohort and reveals significant, yet limited, overlap in differentially abundant mRNAs. a, *Principal component analysis on top 500 most variable mRNAs shows distinct clustering of most cancer and control samples (variance stabilizing transformation DESeq2).* **b,** *Overlap between differentially abundant mRNAs detected in individual cancer-control comparisons. Circles are proportional to the number of genes.* **c,** *Overlap between differentially abundant genes in prostate cancer versus control for the pan-cancer and three-cancer cohort. Fisher's exact test: p=2.9E-52, odds ratio=12.2, Jaccard index=8.3% for higher abundant mRNAs in cancer versus control (higher); p=1.1E-155, odds ratio=59.3, Jaccard index=14.3% for lower abundant mRNAs (lower). Circles are proportional to the number of genes.* **d,** *Gene set enrichment analysis results for custom tissue and cell type sets. Only pathways of Figure 3a shown. Gene sets with q < 0.05 colored according to normalized enrichment scores (NES).* **e,** *Average fraction of the five most*

abundant cell types and macrophages based on cell type deconvolution. Other: cumulative sum of other cell types. Differential abundance: q<0.05 & |log$_2$ fold change|>1. OV: ovarian cancer; PRAD: prostate cancer; UCEC: uterine cancer.

cfRNA tail genes distinguish cancer samples from controls

Apart from liver cancer and AML, our analyses did not reveal evidence for a tumor or tissue of origin signal among mRNAs that were more abundant in cancer patient versus control plasma. Moreover, higher abundant mRNAs were less recurrent across cancer types and showed lower validation rates between cohorts compared to mRNAs with lower abundance in cancer versus control plasma. Our analyses suggest that the latter represent a systemic immune response rather than a tumor derived signal. Based on these observations, we hypothesized that (tumor derived) cfRNA signals may be heterogeneous among patients, and that classic differential mRNA and pathway abundance analysis between groups may not reveal such non-uniform signals. We therefore decided to investigate cfRNA profiles in individual cancer patients using samples from the three-cancer cohort.

To capture aberrations in the cfRNA profile of an individual cancer patient, we compared the mRNA abundance of a cancer plasma sample to the mRNA abundance distribution in the entire control group, that served as a reference. More specifically, a z-score was calculated for each mRNA based on the mean and standard deviation of the log$_2$ normalized count distribution in the control group. Abundant mRNAs with an absolute z-score of at least 3 were defined as "tail genes" for that patient, referring to their position in one of the tails of the control z-score distribution (**Figure 5**a).

We searched for tail genes in each cancer patient from the three-cancer cohort (where we could take advantage of a large control group) and in each control sample, always using all other control samples as reference (Supplemental Figure 12). We identified a total of 3312 unique tail genes in this cohort and observed a significantly higher number of tail genes in plasma samples from cancer patients compared to controls (Kruskal-Wallis p=0.0012, effect size=0.222, **Figure 5**b). 74% of the tail genes were not identified as differentially abundant in cancer samples versus controls (**Figure 5**c). Moreover, for 40.0% of cancer sample tail genes that were differentially abundant between cancer and controls, the direction (i.e. positive or negative z-score) in at least one cancer sample was opposite to the direction reported by the differential abundance analysis, further highlighting the heterogeneity among patients.

Notably, the recurrence of tail genes was much higher in cancer samples than controls; 98% of the control tail genes were identified in only one control sample while 47% of cancer tail genes were identified in more than one cancer sample (**Figure 5**d).

To determine the significance of the observed results, we randomly swapped sample labels prior to tail gene identification and repeated this procedure 20 times. Doing so, we did not observe a significant difference in number of tail genes between the newly labeled cancer samples and controls in any of the repeats (all Kruskal-Wallis p≥0.05), confirming that an increased number of tail genes is specifically associated with cancer samples.

Tail genes detected in one cancer type showed significant overlap with tail genes detected in another cancer type (Fisher's exact tests p≤5.4E-168, odds ratio: [11.1-15.2]), yet limited similarity (Jaccard index: [19.7-34.8%]) (**Figure 5**e). The 1182 unique control tail genes also showed significant overlap with any of the cancer tail gene subsets (pairwise Fisher exact tests p: [5.9E-15 - 8.5E-32], odds ratio: [2.1-2.5]) with less similarity (Jaccard index: [7.4-11.9%]). 63% of control tail genes were not identified as tail gene in any of the cancer samples.

Seven Cancer Gene Census oncogenes were identified as tail genes ($z>3$) in at least one sample, which is significantly more than expected by chance (Fisher's exact p=0.019, odds ratio=3.13). While most oncogenes were only identified as tail gene in a single sample, *KAT6A* was found in seven cancer samples (4 OV, 2 PRAD, and 1 UCEC) but also in one control sample. Overrepresentation analyses (Supplemental Figure 13, Supplemental Table 5) demonstrated that tail genes that are higher abundant in at least one cancer sample ($z>3$) were involved in different processes including platelet activation and signaling, actin binding and dynamics, and extracellular matrix. Tail genes that are lower abundant in at least one cancer sample ($z<-3$) were mainly related to mRNA splicing and translation. Significantly enriched processes in the cancer tail gene sets were not enriched in the control tail gene set, and processes enriched in the lower abundant (cancer) tail genes showed higher recurrence across the three cancer types compared to those enriched in the higher abundant tail genes.

Given the higher number of tail genes in cancer versus controls, we further assessed the binary (cancer/control) classification potential of the number of tail genes per sample. We first selected a subset of tail genes, further coined biomarker tail genes, that were significantly associated to either the cancer or control state using leave-one-out Fisher exact tests (see Methods for details). This resulted in 108 biomarker tail genes, with a significant difference in number of biomarker tail genes in cancer and control samples (two-sided Wilcoxon rank-

sum p=3.1E-11, effect size=0.845). None of the biomarker tail genes were recurrent tail genes in control samples and 54% were not identified as differentially abundant in any cancer type compared to controls (Supplemental Figure 14). Applying the biomarker tail gene selection strategy to the 20 datasets with randomly swapped sample labels resulted in considerably fewer or no biomarker tail genes at all: between 0 and 7 biomarker tail genes (median: 2) instead of 108.

When selecting biomarker tail genes in a specific cancer group versus controls, we obtained 143 biomarker tail genes for OV, 46 for PRAD, and 13 for UCEC. The difference in number of biomarker tail genes between cancer and control samples per biomarker tail gene subset was more significant than based on all tail genes (two-sided Wilcoxon rank-sum: for OV p=1.1E-7 and effect size=0.864; for PRAD p=5.7E-8 and effect size=0.872; for UCEC p=1.4E-8 and effect size=0.912) (**Figure 5**f). Note that the cancer type-specific biomarker tail gene sets showed significant overlap (Fisher's exact p≤1.8E-3, odds ratio: [10.1-22.6]) with limited similarity (Jaccard index: [2.6-9.9%]) (**Figure 5**h).

We then built a classifier for discriminating cancer and control samples based on the number of biomarker tail genes in a particular sample. Using leave-one-out cross-validation, we obtained perfect binary classification for ovarian or prostate cancer samples and controls (AUC=1.000, based on 143 and 46 biomarker tail genes, resp.), and a high classification performance for uterine cancer samples and controls (AUC=0.917, based on 13 biomarker tail genes) (**Figure 5**g). The classification performance was still high when combining all cancer samples (AUC=0.980, based on 108 biomarker tail genes).

Together, these analyses suggest that individual cancer samples can be distinguished from controls based on the number of biomarker tail genes in their plasma cfRNA profiles.
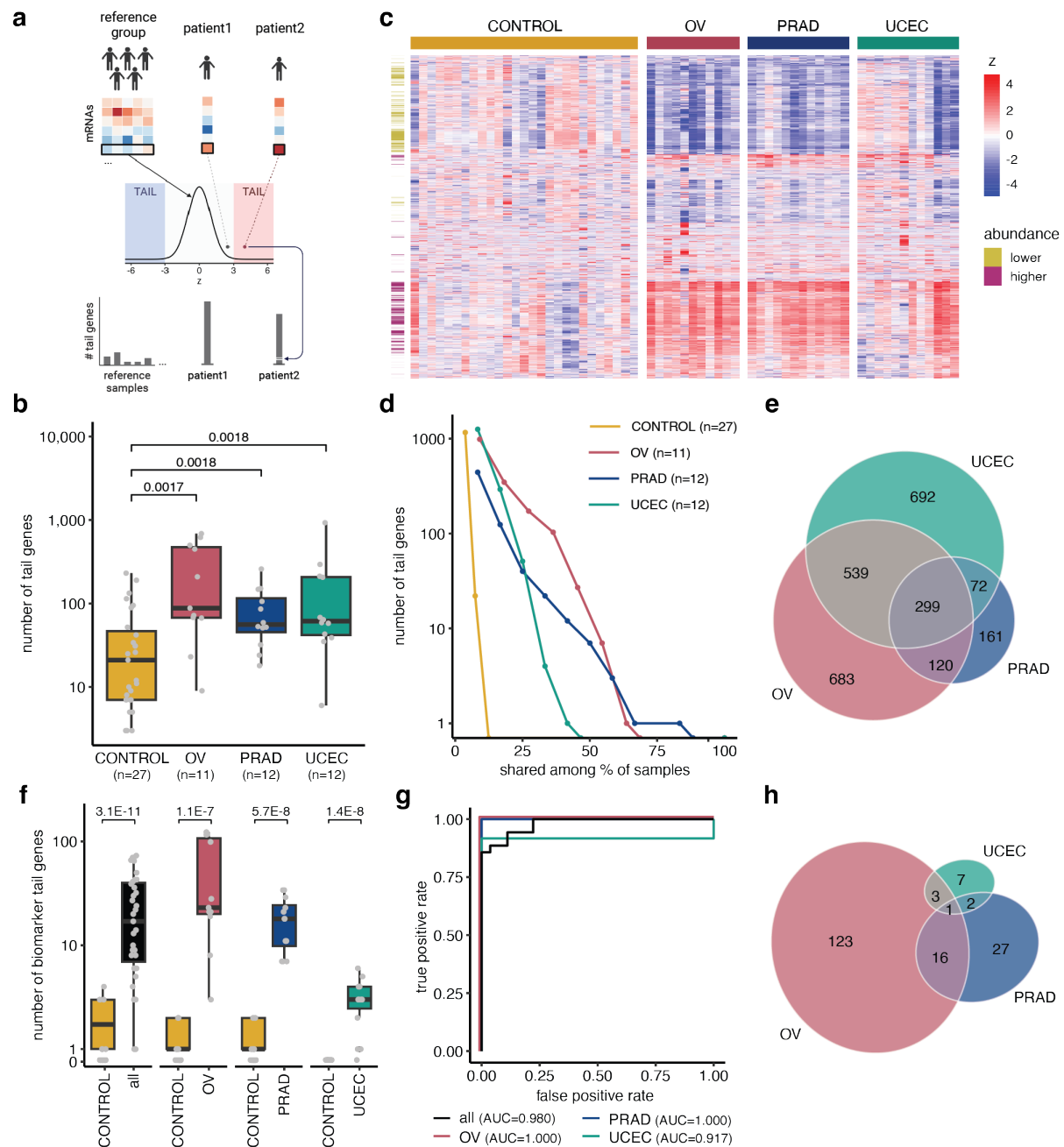
Figure 5: Higher number of tail (biomarker) genes in cancer patient plasma samples compared to controls. a,
*Tail gene identification workflow. A gene in a particular sample for which the abundance deviates more than 3
standard deviations from the reference group abundance distribution is a tail gene for that sample. The number
of tail genes is used as a metric to determine cancer/control status.* **b,** *Boxplot of the number of tail genes per
group, with grey dots representing individual sample counts. Kruskal-Wallis p = 0.001, effect size = 0.222. Two-
sided Wilcoxon rank-sum q-values for specific cancer versus control comparisons indicated in the plot.* **c,** *Z-score
distribution of tail genes in the different samples, all 3312 genes that fulfilled tail gene criteria in at least one of
the samples are shown. For visualization purposes, z-scores above 5 or below -5 were reduced to 5 and -5,
respectively. Genes (rows) clustered based on Euclidean distance.* **d,** *Number of tail genes shared by a certain
fraction of samples of the same type. Number of samples indicated between brackets.* **e,** *Overlap between tail*

*genes detected in the different cancer types. **f,** Boxplot of number of biomarker tail genes per subset in control (CONTROL) versus the respective cancer samples. Total number of biomarker tail genes considered for each comparison: 108 for all cancer (n=35) versus control, 143 for OV versus control, 46 for PRAD versus control, 13 for UCEC versus control. Grey dots represent individual sample counts. Two-sided Wilcoxon rank-sum p-values indicated in plot. **g,** ROC curve of leave-one-out cross-validated classifier for binary cancer/control classification based on the number of biomarker tail genes for control and ovarian cancer samples (OV), prostate cancer samples (PRAD), uterine cancer samples (UCEC), or all cancer samples (all) using the respective biomarker tail gene sets. **h,** Overlap of cancer type-specific biomarker tail genes. Boxplots show lower quartile (Q1), median, and upper quartile (Q3). Whiskers extend from the lower and upper quartile to the smallest and largest value, respectively, within at most 1.5*interquartile range (Q3-Q1) from that quartile. More extreme points are plotted as individual black dots. 62 plasma samples considered in total from 27 cancer-free controls (CONTROL), 11 ovarian cancer (OV), 12 prostate cancer (PRAD), and 12 uterine cancer patients (UCEC).*

To independently validate the classification potential of the number of biomarker tail genes, we generated additional plasma cfRNA profiles (lymphoma cohort), including plasma samples from 22 cancer-free control donors and 43 lymphoma patients, more specifically 30 diffuse large B-cell lymphoma (DLBCL) and 13 primary mediastinal large B-cell lymphoma (PMBCL) patients. We identified 5374 unique tail genes, again with more tail genes in cancer samples compared to controls (Kruskal-Wallis p=2.9E-5, effect size= 0.305, Supplemental Figure 15a). All control tail genes were identified in only one control sample while 45.9% of DLBCL and 44.2% of PMBCL tail genes were identified in more than one DLBCL and PMBCL sample, respectively (Supplemental Figure 15b). When swapping sample labels (20 repeats) prior to tail gene identification, no significant differences in the number of tail genes between cancer and control samples were observed in any of the repeats (Kruskal-Wallis p≥0.05).

Among the tail genes, 297 and 931 were identified as biomarker tail genes using leave-one-out Fisher's exact tests for respectively DLBCL or PMBCL. The number of biomarker tail genes was significantly higher in DLBCL and PMBCL compared to control samples (two-sided Wilcoxon rank-sum: for DLBCL p=3.3E-9, effect size=0.822; for PMBCL p=1.7E-6, effect size=0.811, **Figure 6**a). A binary classifier (cancer/control) based on biomarker tail genes with leave-one-out cross-validation resulted in an AUC of 0.937 and 0.944 for DLBCL and PMBCL, respectively (**Figure 6**b). 78% of the biomarker tail genes were not differentially abundant in any lymphoma subtype versus controls. Notably, early-stage lymphoma patients also displayed an increased number of biomarker tail genes (**Figure 6**c). Cancer diagnosis (i.e. DLBCL or PMBCL) was the only factor significantly associated to the number of biomarker tail

genes (p=1.8E-4 and 3.1E-5 for DLBCL and PMBCL, respectively) in a generalized linear model including diagnosis and tumor stage.

To test if our cancer-control classification strategy based on biomarker tail genes is also applicable to other biofluids, we applied it to a cohort of urine cfRNA profiles (bladder cancer cohort)[14]. This cohort included urine samples of 12 bladder cancer patients (BLCA) and 12 cancer-free control donors. We identified 1152 tail genes of which 39 qualified as biomarker tail gene. The number of biomarker tail genes was significantly higher in bladder cancer versus controls (two-sided Wilcoxon rank-sum p=6.0E-5 and effect size=0.826, **Figure 6**d) and 62% of biomarker tail genes were not differentially abundant between the cancer and control group. In line with the other datasets, sample label swapping prior to tail gene identification did not result in significant differences in the number of tail genes between the newly labeled cancer samples and controls. A binary classifier based on biomarker tail genes with leave-one-out cross-validation resulted in an AUC of 0.903 (**Figure 6**e).

Taken together, our results confirm that the number of biomarker tail genes in blood plasma cfRNA enables accurate classification of cancer patients from controls and suggest that the concept may also be applicable to cfRNA profiles from other biofluids.
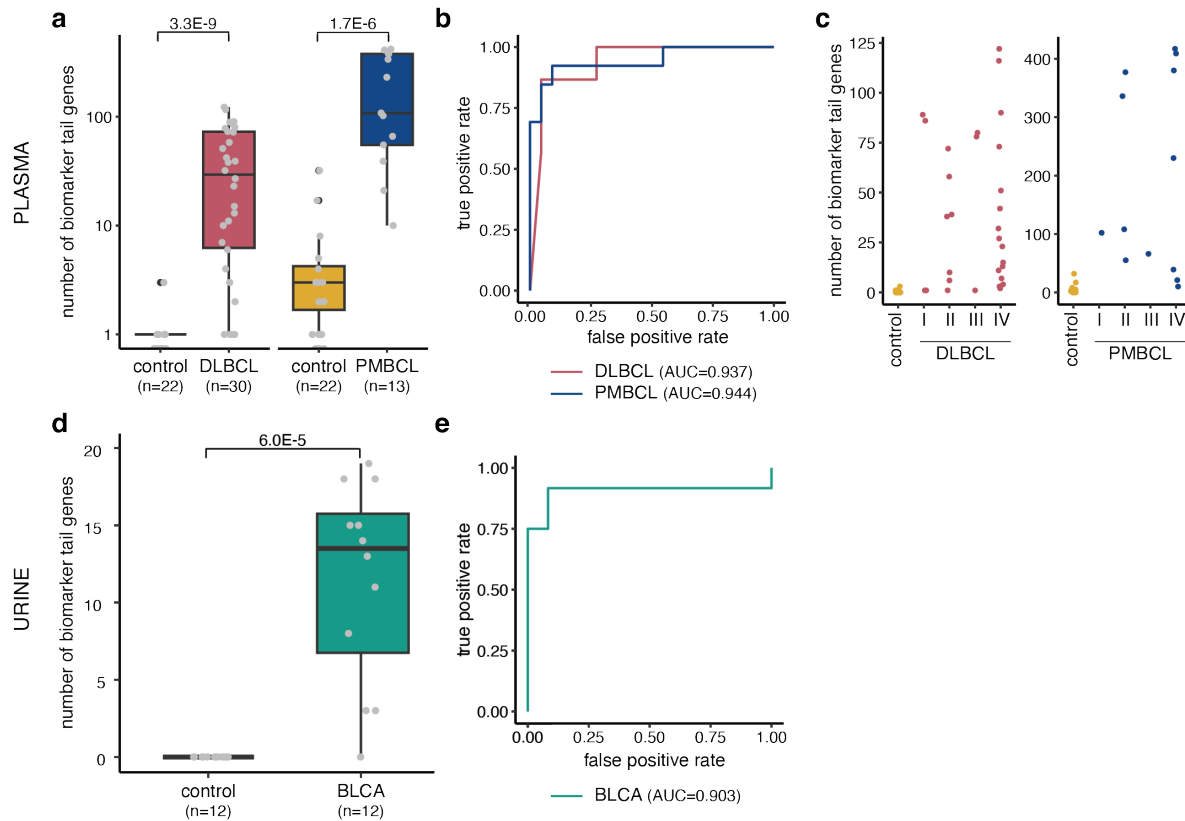
Figure 6: Number of biomarker tail genes is significantly higher in cancer versus control samples in an
***independent blood plasma and urine cohort. a-c**, lymphoma cohort: plasma samples from 22 control, 30 diffuse*
*large B-cell lymphoma (DLBCL), and 13 primary mediastinal large B-cell lymphoma (PMBCL) patients. **a**, Boxplot*
of number of biomarker tail genes in control versus the respective cancer samples. Total number of biomarker
tail genes considered for each comparison: 297 for DLBCL versus control, 931 for PMBCL versus control. Grey dots
*represent individual sample counts. Wilcoxon rank-sum p-values indicated in plot. **b**, ROC curve of leave-one-out*
cross-validated classifier for binary cancer/control classification based on the number of biomarker tail genes for
*control and DLBCL, or control and PMBCL using the respective biomarker tail gene sets. **c**, Number of biomarker*
*tail genes of panel a visualized per cancer stage. **d-e**, bladder cancer cohort: urine samples from 12 control*
*(CONTROL) and 12 bladder cancer (BLCA) patients. **d**, Boxplot of number of biomarker tail genes in control versus*
*cancer samples. 39 biomarker tail genes considered in total. Wilcoxon rank-sum p-value indicated in the plot. **e**,*
ROC curve of leave-one-out cross-validated classifier for binary cancer/control classification based on the number
of biomarker tail genes. Boxplots: lower quartile, median, upper quartile, whiskers of 1.5*interquartile range;
more extreme points are indicated by black dots.

Discussion

In this study, we explored cancer-induced changes in blood plasma cfRNA profiles and investigated if these changes could be exploited for classification purposes. Results from our pan-cancer discovery cohort revealed that AML was the only cancer type for which we found direct evidence for tumor-derived cfRNA in plasma in the form of PML::RARA fusion transcripts. Also, deconvolution of AML plasma cfRNA revealed a high fraction of myeloid progenitor cells, providing additional – albeit indirect – evidence for tumor-derived cfRNA. For solid tumor types, we identified differentially abundant mRNAs in plasma for every cancer versus control comparison, but a cancer type-specific signal was only observed in plasma from liver cancer patients through the enrichment of liver-specific gene sets. Liver is a major contributor to the plasma transcriptome[4] and its high vascularization and blood flow may facilitate mRNA release in blood upon liver cancer progression. Increased cfDNA contributions from the liver have also been observed in liver cancer patients[15]. Note that, despite the enrichment of liver-related mRNAs, the total cfRNA concentration was not increased in plasma from liver cancer patients, indicating that this signal was still strongly diluted.

Considering the organ contribution and dilution argument, other types of liquid biopsies may be better suited to monitor tumor-derived cfRNA for other cancer types. For instance, we could not detect enrichment of prostate tissue-related nor prostate cancer-specific transcripts in blood plasma from prostate cancer patients, in contrast to earlier findings in seminal plasma samples[16].

We did observe several general trends in patients' blood plasma transcriptomes in the pan-cancer cohort, which were confirmed in an independent cohort. The lower abundance of immune-related mRNAs may be linked to the suppressed immune system status in cancer patients. It was recently shown that local tumors can have a systemic impact on the immune system, and that different tumor sites of origin resulted in distinct relative abundances and activity profiles of immune cell types[17]. This may be linked to the observed variations in immune-related mRNA abundance, both between and within cancer types. The (immune) cell-related mRNA contributions agreed with reported cell abundance trends found in blood from several cancer patients[18], with the exception of neutrophil-related mRNAs that are lower abundant in plasma. However, neutrophils can have a dual role in cancer[19] and reduced neutrophil cell-free mRNA abundance may result from neutrophils specifically recruited to

tumor sites. Finally, the negative enrichment of blood/erythrocyte gene sets may be linked to anemia, a common condition in cancer patients. Among the processes that we found positively enriched in cancer patient plasma, some are linked to hallmarks for cancer progression and metastasis, including epithelial-to-mesenchymal transition and increased blood vessel signal that stem from leaky vasculature and angiogenesis[20].

A limitation of the pan-cancer cohort is that control samples were not always perfectly age and sex-matched. The anaplastic astrocytoma, cervical cancer, and testicular germ cell tumor patients were younger as these types predominantly appear at younger age. A dedicated cohort with matched control samples may be better for exposing cancer-related changes in these cancer types. Similarly, while male and female donors were balanced in the control group, this was not always possible for the different cancer types due to sex-specificity (e.g. prostate, testicular, breast, cervical, and ovarian cancer) or sample availability. Nevertheless, at most 4 out of 8 donors were not sex-matched in cancer vs control group comparisons in the pan-cancer cohort, and our main conclusions were not impacted when only using controls of the same sex in the three-cancer cohort. Another limitation is the relatively small sample size per cancer type, which might contribute to false positives and insufficient power to detect true differences.

The variable mRNA abundance in plasma, combined with the limited overlap of differentially abundant mRNAs across cohorts of the same cancer type prompted an alternative approach that can effectively deal with patient heterogeneity. The tail gene concept satisfies this requirement by identifying mRNAs whose abundance in individual samples significantly deviates from the abundance distribution in a reference group. While the dark channel biomarker gene concept[4] is in part based on a more patient-centric approach, it also requires differential abundance at group level to be considered potential biomarkers. Moreover, the dark channel concept specifically looks at genes that are absent (dark) in control samples and therefore cannot capture changes in transcript abundance of genes that are also present in healthy plasma transcriptomes. Of note, 19 dark channel biomarker genes were identified for lung and breast cancer by Larson et al.[4] but five of those genes could be readily detected in control samples from our cohorts, indicating that the "darkness" (i.e. absence of gene transcripts in control samples) should be re-evaluated in different cohorts.

Tail gene counting is a simple metric for classifying samples as cancer or controls. Considering that it is not based on gene signatures with weighted contributions of individual features, we

believe it could be more robust and compatible with observed patient heterogeneity. Nevertheless, it requires a large and representative group of cancer-free control samples. A control group only needs to be established once, if the entire workflow – from sample collection to RNA-sequencing – is standardized across cancer and control samples. This approach should minimize the introduction of batch effects that may skew cfRNA distributions between a pre-established cohort of cancer-free controls and newly profiled cancer or control samples. In this regard, our group has demonstrated that preanalytical variables (blood collection tube, time between blood collection and plasma preparation, RNA extraction kit) can indeed dramatically impact cfRNA profiles[21].

Deviations in the number of tail genes is not necessarily restricted to cancer patients, nor to blood plasma. Indeed, cfRNA from urine provides a good source of biomarker tail genes to identify bladder cancer patients. Other diseases may be characterized by an increase in tail genes, although the specific tail (biomarker) genes may differ. Further studies are needed to examine the applicability and overlap of tail genes in non-malignant disease cohorts. Similarly, while we have preliminary evidence that biomarker tail genes are also significantly more numerous in low stage patients, additional follow-up studies comprising different stages across various cancer types could reveal whether the concept is suited for early-stage cancer screening or monitoring.

Methods

Sample cohorts

The study was approved by the ethics committee of Ghent University Hospital, Belgium (no. B670201734362) and performed in accordance with the Declaration of Helsinki.

Pan-cancer plasma and three-cancer cohort

Blood plasma samples of 266 human donors were obtained from Proteogenex (CA, USA) with informed consent from all donors. The pan-cancer discovery cohort covers 25 different cancer types and a cancer-free control group. For each type, plasma was collected from 8 different donors. The three-cancer cohort consisted of prostate cancer (PRAD), ovarian cancer (OV), and endometrial cancer (UCEC) plasma samples, with 12 donors per type. This cohort also included plasma samples from the 8 control donors of the pan-cancer cohort as well as from 22 additional control donors. For independent validation of pan-cancer results, only the

control samples from the additional control donors were used. For tail gene discovery, all control samples in the three-cancer cohort were used.

All cancer patients in both cohorts had locally advanced (stage 3) to metastatic cancer (stage 4), except for 6 seminoma patients (stage 1). Blood was drawn before treatment with 6 exceptions: 4 glioblastoma patients (grade 4-5) already received chemo and radiation therapy, one prostate cancer patient with metastasis received hormone therapy, and one melanoma patient with metastasis received immunotherapy. Demographic and clinical information can be found in Supplemental Table 1.

Lymphoma cohort

The lymphoma cohort consisted of plasma samples from 65 human donors: 30 DLBCL patients, 13 PMBCL patients, and 22 cancer-free control donors. Plasma samples were collected following approval by the ethics committee of Ghent University Hospital, Belgium (B670201733701), and written, informed consent was obtained from all patients.

Bladder cancer cohort

The bladder cancer cohort is described in more detail elsewhere[14]. This cohort consists of urine samples from 12 muscle-invasive bladder cancer patients and 12 control donors.

Blood collection and plasma preparation

Blood from the pan-cancer and three-cancer cohort donors was collected in EDTA vacutainer tubes (Becton Dickinson, 367525). Blood was stored at 4 °C until plasma preparation which started by gently inverting the EDTA tube 10 times and centrifugating for 10 min at 1500 g (without brake at 4 °C). Supernatans was then transferred to 15 mL centrifuge tubes and centrifuged again for 10 min at 1500 g (without brake at 4 °C). The resulting platelet depleted plasma was transferred to 2 mL cryovials, frozen and stored at -80 °C within 4 hours of blood collection. Plasma samples were shipped on dry ice and only thawed on ice immediately before RNA isolation.

For the lymphoma cohort, 2.5 mL of blood was collected from each donor in PAXgene Blood DNA Tubes (BD Biosciences, 761165). Plasma was prepared by a one-step 15 min centrifugation at 1900 g without brake (room temperature) and stored at -80 °C within 4 hours of blood collection.

RNA isolation and gDNA removal

RNA was isolated from 200 µL of plasma with the miRNeasy Serum/Plasma kit (Qiagen, 217184), according to the manufacturer's instructions. For the pan-cancer and three-cancer cohort, 2 µL Sequin spike-in controls (1/1,300,000 of stock solutions mix A, Garvan Institute of Medical Research, Australia) was added to the lysate during RNA isolation as previously described[22]. For the lymphoma cohort, 2 µL of Sequin spike-in controls were added to the sample lysates (1/5000 of stock solution mix A (Garvan Institute of Medical Research) and 2 µL of External RNA Control Consortium (ERCC) spike-in controls (ThermoFisher Scientific, 4456740) were added to 12 µl RNA eluate.

Genomic DNA was removed by adding 1 µL HL-dsDNase (ArcticZymes, 70800-202) and 1.6 µL reaction buffer (ArcticZymes, 66001) to 12 µL RNA eluate, 10 min incubation at 37 °C, followed by 5 min incubation at 55 °C. RNA was stored at -80 °C and thawed on ice immediately before library preparation.

Messenger RNA capture library preparation, sequencing, and quantification

MRNA capture library preparation in pan-cancer and three-cancer cohorts started from 8.5 µL DNase treated RNA eluate. cDNA synthesis was performed using TruSeq RNA Library Prep for Enrichment (Illumina, 20020189) as previously described[22]. Briefly, RNA was fragmented, and first strand cDNA was generated using random priming. RNA templates were subsequently removed and replaced by a newly synthesized second strand of cDNA. AMPure XP beads (Beckman Coulter Life Sciences, A63881) were used for purifying the blunt-ended double stranded cDNA. 30 µL cDNA of each sample was then used as input for Illumina DNA Prep with Enrichment (previously Nextera Flex for Enrichment; Illumina, 20025524). Tagmentation and amplification steps were done according to manufacturer's instructions. Quality of resulting pre-enriched libraries was assessed using a high sensitivity Small DNA Fragment Analysis Kit (Agilent Technologies, DNF-477-0500). The libraries were randomly pooled per 8 or 6 samples, for the pan-cancer and three-cancer cohort, respectively, based on their relative concentrations determined using qPCR for reference genes YWHAZ, ACTB, B2M, and UBC. Each multiplex pool was concentrated to a volume of 15 µL with AMPure XP beads (Beckman Coulter Life Sciences, A63881). Finally, enrichment was performed using probes from the Illumina Exome Panel (Illumina, 20020183), probes complementary to the spike-in controls, and blocking probes against globin (anti-CEX) as previously described[22]. At

the end of the enrichment workflow, equimolar library pools were prepared based on qPCR quantification with KAPA Library Quantification Kit (Roche Diagnostics, KK4854).

Paired-end sequencing of both cohorts was performed (2x100 nucleotides) on a NovaSeq 6000. For the pan-cancer cohort, a NovaSeq S2 kit (Illumina, 20028315) was used with standard workflow loading of 1.55 nM (1% PhiX). For the three-cancer cohort, a NovaSeq S1 kit (Illumina, 20028318) was used with Xp workflow loading of 1.25 nM (2% PhiX).

Adapter trimming and removal of reads shorter than 20 nucleotides was done with cutadapt (v1.18). Read quality was assessed with FastQC (v0.11.9) and low-quality reads were filtered: only reads where at least 80% of bases in both mates have a quality score ≥20 (99% accuracy) were kept (between 87 and 99% of reads/sample). Samples with very few reads (< 2M) were removed from all analyses. More specifically, 4 samples were removed in the pan cancer plasma cohort (1 lymphoma, 1 bladder, 1 head and neck, and 1 lung cancer sample) and 4 samples in the three-cancer cohort (3 control samples, of which 1 repeated from first cohort, and 1 ovarian cancer) as indicated in Supplemental Table 1. Quality filtered reads were then mapped with STAR[23] (v2.6.0) using the default parameters (except for --twopassMode Basic, --outFilterMatchNmin 20 and --outSAMprimaryFlag AllBestScore). The reference files for all analyses were based on genome build GRCh38 and transcriptome build Ensembl v91, complemented with spike annotations. Finally, gene counts were determined with HTSeq[24] (v0.11.0) in non-stranded mode, only considering uniquely mapping reads.

Total RNA library preparation, sequencing, and quantification

Total RNA sequencing libraries of the lymphoma cohort were prepared starting from 8 µL of RNA eluate using the SMARTer Stranded Total RNA-Seq Kit v3 – Pico Input Mammalian (Takara, 634487) according to the manufacturer's protocol. Equimolar library pools were prepared based on qPCR quantification with KAPA Library Quantification Kit (Roche Diagnostics, KK4854). The libraries were paired-end sequenced (2x100 nucleotides) on a NovaSeq 6000 instrument using a NovaSeq S2 kit (Illumina, 20028315) with standard workflow loading of 0.65 nM (2% PhiX).

After adapter trimming with cutadapt (v1.18) and quality control with FASTQC (v0.11.9), reads were mapped with STAR[23] (v2.7.3) using default options and the GRCh38 reference described above. Resulting BAM files were deduplicated using UMI-tools (v1.0.0) based on the unique molecular identifier (UMI) sequences in the Pico v3 SMART UMI adapters. Gene

counts were determined with HTSeq[24] (v0.11.0) in reverse stranded mode, only considering uniquely mapping reads.

Data analyses

Most data processing and visualization was done in R (v4.2.1) using tidyverse (v1.3.2) and pheatmap (v1.0.12). Other tools and R packages used for specific analyses are mentioned below. Color schemes are based on Paul Tol's technical note[25].

Detection threshold

To remove noisy datapoints, we applied a threshold of at least 10 counts. This threshold was based on the median threshold that removes at least 95% of single positive genes[26] - genes that have counts in one replicate but not in the other - between control samples.

MRNA concentration

MRNA concentration was determined as previously described[22]. Briefly, the mass of a specific Sequin spike-in control was calculated based on the input concentration and volume of spike-in mix added to the sample. The corresponding mRNA concentration was then estimated by multiplying the spike mass by the ratio of reads mapped to the human genome versus the number of reads mapped to the specific spike, and finally dividing the obtained mass by the plasma volume of the sample. In this study, all spikes above detection threshold were considered and the geometric mean per sample was taken as the sample's mRNA concentration.

Fusion gene detection

FusionCatcher[27] (v1.30) was used with default settings for fusion transcript identification. Stringent filtering was applied to exclude potential false positives: transcripts with a FusionCatcher label indicative for false positives, transcripts with reads simultaneously mapping to both fusion partners, and transcripts with fusion partners less than 100 kbp apart were filtered out. Only exon-exon fusions were included and detected fusions in plasma were compared to fusions in the Fusion Gene annotation DataBase (FusionGDB)[28], focusing on fusion genes identified in tissue samples of The Cancer Genome Atlas[29].

Differential abundance and principal component analysis

DESeq2 (v1.36.0) was used for normalization and differential abundance analysis. MRNAs were pre-filtered by requiring gene counts equal to or greater than the detection threshold in at least half of the tumor or half of the control samples. In the DESeq2 result table, genes with a Benjamini-Hochberg corrected p-value (q) below 0.05 and an absolute $\log_2$ fold change

above 1 were considered differentially abundant. Principal component analysis was performed with DESeq2 plotPCA on the 500 most variable genes after applying variance stabilizing transformation. Volcano plots were visualized using EnhancedVolcano (v1.14.0) and area-proportional Euler diagrams were made using eulerr (v6.1.1). Differential abundance analysis results are freely available at Zenodo (doi:10.5281/zenodo.7953707).

Gene set enrichment and overrepresentation

Fgsea[30] (v1.22.0) was used for preranked gene set enrichment analysis based on $\log_2$ transformed fold changes between cancer and controls obtained from DESeq2 differential abundance analysis. Significant enrichment was defined by a false discovery rate ≤ 0.05. Hallmark[9] and Canonical Pathways gene sets derived from Kyoto Encyclopedia of Genes and Genomes (KEGG)[10], http://www.pathway.jp, were obtained via the Molecular Signatures Database, MSigDB (v2022.1)[31]. Besides these MSigDB gene sets, custom tissue and cell type specific gene sets were made using inhouse and external references as described below. Gene set enrichment analysis results and custom gene sets are available at Zenodo (doi:10.5281/zenodo.7953707). Functional analysis of mRNA sets was done using the functional annotation tool of DAVID (v2021)[32,33] and - for custom gene sets - the fora function of fgsea. For each functional analysis, a background was provided which included all mRNAs satisfying the count threshold in at least one sample.

RNA Atlas cell type gene sets

These cell type gene sets were defined based on total RNA sequencing data of cells and cell lines in the RNA Atlas[34]. Protein coding gene inclusion criteria were an expression of at least 16 counts after variance stabilizing transformation and an expression fold change of at least 10 compared to the cell type with second highest expression. 15 out of 32 defined cell type sets included more than 5 genes.

Tabula Sapiens cell type gene sets

These cell type gene sets were based on the Tabula Sapiens v1 basis matrix defined by Vorperian et al[2]. Protein coding genes with at least 5 CPM and an expression fold change of at least 10 compared to the cell type with the second highest expression were retained. 13 out of 39 defined cell type gene sets included more than 5 genes.

GTEX tissue gene sets

These tissue gene sets were defined using SPECS specificity scores[35] of GTEx[36] tissue samples, summarized in https://specs.cmgg.be. Criteria for protein coding gene inclusion in a certain tissue gene set were a SPECS score ≥ 0.98 and a median TPM ≥ 5. Large gene sets were reduced to the top 200 genes based on the highest SPECS score. 23 out of 27 defined tissues gene sets included more than 5 genes.

HPA-RNA Atlas tissue gene sets

These tissue gene sets were defined based on expression data from the Human Protein Atlas[37] (HPA, v18, https://v18.proteinatlas.org/) in combination with total RNA-sequencing data from the RNA Atlas[34]. Human Protein Atlas protein coding genes needed to have a TPM value of at least 5 and expression that is at least 10 times higher in the tissue with highest expression compared to the tissue with second highest expression. These genes sets were further finetuned by only keeping those genes with the highest expression in the same tissue in the RNA Atlas dataset. Finally, large gene sets were reduced to the top 200 genes based on the highest fold changes. 15 out of 18 defined tissue gene sets included more than 5 genes.

TCGA cancer tissue gene sets

These gene sets were defined similarly to the GTEX gene sets but using expression in The Cancer Genome Atlas (TCGA) cancer tissue samples, generated by the TCGA Research Network: https://www.cancer.gov/tcga. Protein coding genes with a SPECS score of at least 0.98 in a certain tissue were included in the gene set with a limit of 200 genes, based on highest SPECS score. 19 out of 23 defined cancer tissue gene sets included more than 5 genes.

Cell type deconvolution

NuSVR deconvolution using the Tabula Sapiens v1 basis matrix was performed as described by Vorperian et al.[2] and the accompanying GitHub repository, https://github.com/sevahn/deconvolution. As recommended by the authors, data was CPM normalized and no log transformation was performed. Note that the erythrocyte fraction is underestimated due to the absence of hemoglobin probes in mRNA capture sequencing.

Tail genes

To identify tail genes, transcript counts of every sample were first converted to a customized z score based on the mean and standard deviation in the reference group, including all control samples except the sample of interest. More specifically, a pseudocount was added to all

normalized transcript counts followed by log_2 transformation. Then, for each gene, the mean and standard deviation of these transformed counts in the reference group was used to scale the transformed counts in the sample of interest.

Tail genes were then defined as genes with at least 40 counts after DESeq2 normalization and deviating more than 3 standard deviations from the mean of the control reference ($|z|>3$). For each gene in a sample of interest:

$$zscore_{gene} = \frac{log_2\big(normalized\ counts_{gene} + 1\big) - \overline{ref_{gene}}}{SD_{ref_{gene}}}$$

where $\overline{ref_{gene}}$ and $SD_{ref_{gene}}$ are respectively the mean and standard deviation of log_2 transformed counts for this gene over all (other) control samples.

Fisher's exact tests (based on $|z|>3$ and donor cancer/control status) were used to select a subset of tail genes, named biomarker tail genes, that are specifically associated to the disease state. To avoid selection being biased by individual samples, Fisher's exact testing for each tail gene was done iteratively, each time leaving out a different sample, and a tail gene needed to be significant ($p<0.05$) in every iteration to be called a biomarker tail gene. As a result, the tail gene needs to be recurrent in at least two samples.

Binary logistic regression, R glm function with binomial family, was used to classify a sample as cancer or control based on the number of biomarker tail genes. Leave-one-out cross-validation was used by iteratively leaving out a different sample from the training set and testing the model on this sample. Based on these predictions, the Receiver Operating Characteristic (ROC) curve and Area Under Curve (AUC) were calculated and visualized using pROC (v1.18.0)[38].

For internal validation, all sample labels were randomly reshuffled using the sample function in R without replacement. Next, tail gene identification and evaluation was repeated based on the new class labels (using the new control samples as reference). This process was repeated 20 times.

Statistics

Kruskal-Wallis tests were used to compare multiple groups, and Wilcoxon rank-sum tests were used to compare two groups. Corresponding statistical significance and effect sizes were calculated with rstatix (v0.7.2). For individual testing, p-values smaller than 0.05 were considered significant. In case of multiple testing, the Benjamini-Hochberg procedure was

used to calculate false discovery rate adjusted p-values (q-values) and significance was defined as q smaller than 0.05.

Significance of overlap between gene sets was determined by Fisher's exact test in GeneOverlap (v1.32.0). The universe consisted of all genes considered for the corresponding differential abundance or tail gene analyses (see filtering above). A Jaccard index was calculated to assess similarity between the gene sets, with 0% indicating no similarity and 100% indicating identical sets.

Data availability

Raw RNA-sequencing data is available under restricted access (access can be requested) in the European Genome-phenome Archive (EGA) to preserve individuals' privacy and comply with patient consent for data sharing under the European General Data Protection Regulation. The pan-cancer and three-cancer cohort FASTQs can be found under study EGAS00001006755 (dataset EGAD00001009713). The lymphoma cohort FASTQs can be found under study EGAS00001007127 (dataset EGAD00001010259). The bladder cancer cohort FASTQs can be found under study EGAS00001003917 (dataset EGAD00001005439). Differential abundance and gene set enrichment analysis results are available (open access) in a Zenodo repository (doi:10.5281/zenodo.7953707).

Code availability

Code for differential abundance and tail gene analyses is available on GitHub at https://github.com/OncoRNALab/tailgenes.

Acknowledgements

Funding

Conflict of interest

A.M., J.V. and P.M. are inventors on a patent application regarding the tail gene concept.

References

1. Pessoa, L. S., Heringer, M. & Ferrer, V. P. ctDNA as a cancer biomarker: A broad overview. *Critical Reviews in Oncology/Hematology* **155**, 103109 (2020).

2. Vorperian, S. K., Moufarrej, M. N. & Quake, S. R. Cell types of origin of the cell-free transcriptome. *Nat Biotechnol* **40**, 855–861 (2022).

3. Moufarrej, M. N. *et al.* Early prediction of preeclampsia in pregnancy with cell-free RNA. *Nature* **602**, 689–694 (2022).

4. Larson, M. H. *et al.* A comprehensive characterization of the cell-free transcriptome reveals tissue- and subtype-specific biomarkers for cancer detection. *Nat Commun* **12**, 2357 (2021).

5. Chen, S. *et al.* Cancer type classification using plasma cell-free RNAs derived from human and microbes. *eLife* **11**, e75181 (2022).

6. Roskams-Hieter, B. *et al.* Plasma cell-free RNA profiling distinguishes cancers from pre-malignant conditions in solid and hematologic malignancies. *npj Precis. Onc.* **6**, 1–11 (2022).

7. Bryzgunova, O. E., Konoshenko, M. Y. & Laktionov, P. P. Concentration of cell-free DNA in different tumor types. *Expert Review of Molecular Diagnostics* **21**, 63–75 (2021).

8. Liquori, A. *et al.* Acute Promyelocytic Leukemia: A Constellation of Molecular Events around a Single PML-RARA Fusion Gene. *Cancers (Basel)* **12**, 624 (2020).

9. Liberzon, A. *et al.* The Molecular Signatures Database (MSigDB) hallmark gene set collection. *Cell Syst* **1**, 417–425 (2015).

10. Kanehisa, M. & Goto, S. KEGG: Kyoto Encyclopedia of Genes and Genomes. *Nucleic Acids Research* **28**, 27–30 (2000).

11. Khwaja, A. *et al.* Acute myeloid leukaemia. *Nat Rev Dis Primers* **2**, 1–22 (2016).

12. Giannakeas, V. *et al.* Analysis of Platelet Count and New Cancer Diagnosis Over a 10-Year Period. *JAMA Network Open* **5**, e2141633 (2022).

13. Haemmerle, M., Stone, R. L., Menter, D. G., Afshar-Kharghan, V. & Sood, A. K. The Platelet Lifeline to Cancer: Challenges and Opportunities. *Cancer Cell* **33**, 965–983 (2018).

14. Hulstaert, E. *et al.* Charting Extracellular Transcriptomes in The Human Biofluid RNA Atlas. *Cell Reports* **33**, 108552 (2020).

15. Sun, K. *et al.* Plasma DNA tissue mapping by genome-wide methylation sequencing for noninvasive prenatal, cancer, and transplantation assessments. *Proceedings of the National Academy of Sciences* **112**, E5503–E5512 (2015).

16. Hulstaert, E. *et al.* Exploring the extracellular transcriptome in seminal plasma for non-invasive prostate cancer diagnosis. 2021.05.11.21256306 Preprint at https://doi.org/10.1101/2021.05.11.21256306 (2021).

17. Allen, B. M. *et al.* Systemic dysfunction and plasticity of the immune macroenvironment in cancer models. *Nat Med* **26**, 1125–1134 (2020).

18. Hiam-Galvez, K. J., Allen, B. M. & Spitzer, M. H. Systemic immunity in cancer. *Nat Rev Cancer* **21**, 345–359 (2021).

19. Xiong, S., Dong, L. & Cheng, L. Neutrophils in cancer carcinogenesis and metastasis. *Journal of Hematology & Oncology* **14**, 173 (2021).

20. Lugano, R., Ramachandran, M. & Dimberg, A. Tumor angiogenesis: causes, consequences, challenges and opportunities. *Cell. Mol. Life Sci.* **77**, 1745–1770 (2020).

21. Consortium, exRNAQC *et al.* Performance of RNA purification kits and blood collection tubes in the Extracellular RNA Quality Control (exRNAQC) study. 2021.05.11.442610 Preprint at https://doi.org/10.1101/2021.05.11.442610 (2021).

22. Hulstaert, E. *et al.* Messenger RNA capture sequencing of extracellular RNA from human biofluids using a comprehensive set of spike-in controls. *STAR Protocols* **2**, 100475 (2021).

23. Dobin, A. *et al.* STAR: ultrafast universal RNA-seq aligner. *Bioinformatics* **29**, 15–21 (2013).

24. Anders, S., Pyl, P. T. & Huber, W. HTSeq—a Python framework to work with high-throughput sequencing data. *Bioinformatics* **31**, 166–169 (2015).

25. Tol, P. Colour Schemes, Technical Note SRON/EPS/TN/09-002. (2012).

26. Mestdagh, P. *et al.* Evaluation of quantitative miRNA expression platforms in the microRNA quality control (miRQC) study. *Nature Methods* **11**, 809–815 (2014).

27. Nicorici, D. *et al.* FusionCatcher – a tool for finding somatic fusion genes in paired-end RNA-sequencing data. 011650 Preprint at https://doi.org/10.1101/011650 (2014).

28. Kim, P. & Zhou, X. FusionGDB: fusion gene annotation DataBase. *Nucleic Acids Research* **47**, D994–D1004 (2019).

29. Gao, Q. *et al.* Driver Fusions and Their Implications in the Development and Treatment of Human Cancers. *Cell Reports* **23**, 227-238.e3 (2018).

30. Korotkevich, G. *et al.* Fast gene set enrichment analysis. 060012 Preprint at https://doi.org/10.1101/060012 (2021).

31. Subramanian, A. *et al.* Gene set enrichment analysis: A knowledge-based approach for interpreting genome-wide expression profiles. *Proceedings of the National Academy of Sciences* **102**, 15545–15550 (2005).

32. Huang, D. W., Sherman, B. T. & Lempicki, R. A. Systematic and integrative analysis of large gene lists using DAVID bioinformatics resources. *Nat Protoc* **4**, 44–57 (2009).

33. Sherman, B. T. *et al.* DAVID: a web server for functional enrichment analysis and functional annotation of gene lists (2021 update). *Nucleic Acids Res* **50**, W216–W221 (2022).

34. Lorenzi, L. *et al.* The RNA Atlas expands the catalog of human non-coding RNAs. *Nat Biotechnol* **39**, 1453–1465 (2021).

35. Everaert, C., Volders, P.-J., Morlion, A., Thas, O. & Mestdagh, P. SPECS: a non-parametric method to identify tissue-specific molecular features for unbalanced sample groups. *BMC Bioinformatics* **21**, 58 (2020).

36. Lonsdale, J. *et al.* The Genotype-Tissue Expression (GTEx) project. *Nat Genet* **45**, 580–585 (2013).

37. Uhlén, M. *et al.* Tissue-based map of the human proteome. *Science* **347**, 1260419 (2015).

38. Robin, X. *et al.* pROC: an open-source package for R and S+ to analyze and compare ROC curves. *BMC Bioinformatics* **12**, 77 (2011).